CEES 2020
12 – 15 OCTOBER 2021
COIMBRA | PORTUGAL
INTERNATIONAL CONFERENCE
CONSTRUCTION, ENERGY
ENVIRONMENT & SUSTAINABILITY

FITNESS OF A HIGH-CALCIUM SLAG FOR THE PRODUCTION OF ALKALI ACTIVATED MATERIALS.

Omar Alelweet[1]
Sara Pavia[1]

[1] Department of Civil Engineering, University of Dublin Trinity College
[2] Department of Civil Engineering, University of Dublin Trinity College
Corresponding author: pavias@tcd.ie

Keywords
Ground Granulated Blastfurnace Slag (GGBS), alkali activation, devitrification, amorphousness, strength.

Abstract
Alkali-activated (AA) materials are considered a more sustainable alternative to some traditional materials. This paper studies the feasibility of producing building materials by activating an Irish ground granulated blast furnace slag (GGBS) with a range of alkali metal activators. The results indicate that the GGBS can be successfully used for the production of AA materials. The slag is ultra-fine, basic and highly amorphous, with CaO/SiO_2 and Al_2O_3/SiO_2 ratios that are considered suitable for alkali-activation. The chemical composition complies with the standard requirements for the use of slags in concretes, mortars and grouts. The slag is totally amorphous, hence devitrification was required to determine its mineral composition. Devitrification evidenced that the composition concurs with that of other active slags (a melilite-gehlenite isomorphous solution) indicating a high reactivity. Cracking due to drying shrinkage is one of the challenges of AA materials, but the high Ca content of the Irish slag has likely reduced drying-shrinkage cracking, providing a generally sound microstructure.

The thermal tests results support the chemical and mineralogical analyses indicating that the GGBS has neither organic carbon nor carbonates. In addition, the heat evolution in the calorimetric tests mirrors the evolution of the glass and the crystalline phases determined with X-ray diffraction on devitrification. It is clear that most of the glass becomes crystalline between 500 and 800°C, and that the steady heat absorbed in this segment (endothermic curve) is due to the decomposition of the glass to form merwinite and gehlenite.

The slag was activated with sodium hydroxide (NaOH), and sodium silicate (Na_2SiO_3), both combined and separately, to produce mortars. The mortars obtained show reasonable setting times and minimal loss of workability. The strengths are lower than those in the literature, however, the Na_2SiO_3+NaOH activated GGBS shows values suitable for a wide range of applications. The main reason for the strength loss when using the Na_2SiO_3 activator is mainly an excessive $\%Na_2O$ by mass of slag, while the reason for the strength loss when the NaOH activator is involved is an elevated alkalinity. The strength results and the microstructural analyses evidenced that rising curing temperature improves the microstructure and the mechanical properties of the Na_2SiO_3+NaOH activated GGBS. It seems from the results, that the GGBS analysed is too fine for a successful activation with Na_2SiO_3 alone, and too reactive for high alkali hydroxide concentrations. The best activator is likely a combination of Na_2SiO_3 and a low molarity (<6M) alkali hydroxide.

1. INTRODUCTION

Alkali-activated materials (AAMs) have been proposed as a more sustainable alternative to traditional Portland cement (PC) products. AAMs can be produced with low carbon emissions and low raw material and fossil fuel consumption. Their reduction in emissions when compared with PC, and the use of waste materials as precursors for their production, may now become the trigger for their wide uptake in the markets. They consist of a silicate precursor which is activated with an alkali-metal and mixed with an aggregate. The precursors are either natural or man-made aluminosilicates, and they can be either cementitious materials with hydraulic properties or pozzolanic. This research uses Irish GGBS as a precursor. It is activated with sodium hydroxide (NaOH), and sodium silicate (Na_2SiO_3) which are considered as best activators according with the literature [1-3]. The alkali solution dissolves the slag generating Si^{4+}, Al^{3+} and Ca^{2+} cations that become available to form a C-A-S-H type gel which is the main reaction product, a C-S-H cement with a high level aluminium substitution [1-3].

Slags have been used for the production of AAs for decades. They were patented in 1958 and used in construction in 1960 in USSR, and precast slag products were used in Eastern Europe, Finland and France in the past [4]. Some AAMs show advantages over PC products including: early hardening, high strengths, lower hydration heat, better resistance to water solubility, chemical attack and carbonation, higher resistance of interfaces and a higher resistance to frost action [3]. However, they face obstacles in the market. They do not include PC binders therefore don't meet existing standards, and they can show too rapid setting, high shrinkage, expansive alkali-aggregate reactions, and salt efflorescence [3]. In particular, AA slags generally show early strength and resistance to sulfates and chlorides [4]. However, disadvantages sometimes include unpleasant handling, skin irritation, inconvenience of mixing more than 2 components, sticky consistency, short setting times, efflorescence, vulnerability to carbonation and tendency to ASR (alkali-silica reaction) [4].

Some of the challenges for alkali-activated cements and concretes are comprehensively and clearly summarised in Shi et al. (2006) [1] including: The appearance of alkali carbonate efflorescence due to the leaching of alkalis and their reaction with the CO_2 in the air; the cracking due to drying shrinkage (which increases as the lime content in the system lowers); and the potential expansion by alkali‑aggregate reaction. The authors raise a further challenge as the typical PC chemical admixtures might not be compatible with alkali-activated materials [1]. Shrinkage can prevent a wider range of applications for alkali-activated materials. Although for certain activators such as fly ash, it could be reduced significantly with heat curing, shrinkage needs to be better explored and understood [2].

As highlighted by previous authors [1-3], the chemical and physical characteristics of the raw materials (which vary from source to source) need to be determined and controlled in order to ensure the quality of alkali-activated materials, and one of the constrains that inhibit the worldwide, large-scale production of alkaline cements is the non-uniformity of the raw materials required to manufacture them. Furthermore, in alkaline cement design, the activator chosen is essential as it determines the properties and durability of the final product. Hence, the activator needs to be chosen based on the chemical composition and physical-chemical properties of the raw material [2-3].

This paper intends to contribute to this important quality control by investigating the composition and properties of an Irish slag, as a potential raw material for the production of alkali activated cements. It also studies different alkali activators, in an effort to determine how this slag can be best activated. The paper also investigates the micro and macrostructure of the resultant materials, with a focus on strength and the effect of curing, as well as the presence of cracking shrinkage and efflorescence.

Alkali activation of slags. Fernández–Jiménez et al. [5] proved that the nature of the alkaline activator is the most significant factor in the development of mechanical strength, overriding the effects of specific surface area of the slag, curing temperature and activator concentration. When the alkali and the precursor are mixed, the pH controls the reactivity because it determines the dissolution of the precursor. According to previous authors, alkali silicate and hydroxide activators are the best activators for slags because they generate the highest pH (or alkalinity) which accelerates the reaction between the activator and the precursor [1-3]. Hydroxide activators induce the hydrolysis of the Si-O-Si and Al-O-Al bonds releasing Si^{4+} and Al^{3+}, and provide more hydroxyls which raise the PH to the values required for the dissolution of the precursor. However, it has been noted that silicate activators provide a much higher level of available alkalinity over longer periods because, when a moderate amount of silica dissolves, the PH does not drop rapidly (as it is the case with hydroxide activators) [3].
A high pH is not considered suitable for Ca-rich precursors such as GGBS, because at very high OH- concentrations, although silica and alumina increase solubility calcium becomes less soluble [2]. Therefore, high Ca slags (Ca=35-45%) are usually activated under moderated alkaline conditions [1, 5, 6]. Furthermore, high concentrations of hydroxide activator in GGBS have been reported to encourage efflorescence and increase cost [2-3]. It is considered in the literature that slags can be successfully activated with a combination of alkali hydroxide and silicate. The fluidity of the hydroxide activator maintains a suitable rheology while the silicate activator provides Si ions for the generation of cementing hydrates that contribute to strength [2]. The proportion of NaOH / Na_2SiO_3 is essential as NaOH acts as dissolvent while Na_2SiO_3 acts as a binder [7].

Curing of alkali activated slags. It is well known that the reactions of the non-clinker materials in AAMs are slower than those in PC materials, and that the binding of water is generally slower and /or weaker than in the Ca rich CSH phases of PCs. Therefore, it is even more important to control the curing conditions in AA binders [3]. Curing temperature has been considered an important parameter in the literature, and it is the most widely investigated. However, the optimal curing temperature depends on the slag and the mix design, and it is generally agreed that an extended period of curing is also important to develop a durable material. Curing temperature strongly influences strength development of alkali-activated slag mortars, with significant retardation at 5°C, and significant acceleration at 40°C compared with curing at 20°C [8]. Heat curing promotes high early strength of alkali-activated slag materials, but the strength at later ages is significantly reduced when compared with the material cured at room temperature [9]. Bakharev et al. [9] note that curing at 60°C is the most effective method for sodium silicate activated slags. The authors also note that when slags are activated with a combination of sodium silicate and sodium hydroxide, curing at 70°C accelerates early strength development but, after 28 days, the strength is 35-45% lower than the strength of ambient-cured specimens. However, Altan and Erdoğan [10] observed that AA slags activated with a mixture of sodium hydroxide and sodium silicate, cured at room temperature for a sufficiently long time will reach the same strength or greater than when cured at 80°C.
This paper studies the feasibility of producing AA binders using Irish GGBS. It investigates alkali-activated GGBS mortars produced according to the best outcomes of background research and compares them with PC activated slag and other AA- GGBS materials in the literature.

2. MATERIALS AND METHODS

Mixing, casting and curing. A GGBS made in Ringsend, Ireland, with raw molten slag imported from Europe and a particle density of 1.80 Mg/m^3 was used. The slag was activated with sodium hydroxide (NaOH 8M) and sodium silicate (Na_2SiO_3). The silicate, known as waterglass in the literature, comes as a commercial solution while the NaOH comes in solid form. Using the solid NaOH, an 8M alkali solution was made. The activators were investigated separately and together (Table 1). The objective of mixing the silicate solution with the NaOH alkali solution was to provide extra Silicon ions in the activation process. As aforementioned, this has been claimed in the literature to enhance the mechanical properties. The Na_2SiO_3 /NaOH activator was prepared, at a mass ratio of 1.5, based on a higher compressive strength reported by previous authors [11]. The 0.47 / 0.60 % by weight (Table 1) is the ratio between liquid and solid (alkaline solution / GGBS) that provides a good workability as determined with the initial flow test. As explained below, the amount of alkali solution required for the GGBS to provide a suitable workability for handling and placing was measured with the initial flow diameter test, using a flow table, according to EN 1015-3 [12].
The GGBS and sand were dry mixed at a ratio of 1 to 3 for 6 min, and later in a mixer for a further 3 min. The activator solution was then added and mixed for a further 5 mins. All the activators were in liquid form when added. NaOH was the most viscous and Na_2SiO_3 the stickiest. The filled moulds were vibrated according to the standards, and then the specimens sealed with a plastic sheet to prevent the loss of moisture during curing. The specimens were demoulded after 24 hours and cured in ambient conditions for 24 hours. After this, some of the specimens were cured in an oven, at 60°C for 24 h, and in ambient conditions for the rest of the time.

Table 1. Composition of the alkali activated GGBS mortars.

	GGBS (g)	Sand (g)	Na_2SiO_3 /NaOH	8M NaOH (g)	Na_2SiO_3 (g)	Alkali solution/GGBS (%)
Na_2SiO_3/NaOH	500	1500	1.5	94	141	0.47
NaOH	500	1500	-	117.5	0	0.47
Na_2SiO_3	500	1500	-	0	300	0.60

Workability. Several authors have demonstrated that the rheology of AA slag pastes depends on the activator used [1-3]. As aforementioned, the alkali solution content was adjusted for the mixes to provide a workable mix with a flow diameter of c.175 mm which was deemed as providing a good workability. The NaOH as well as the Na_2SiO_3 + NaOH activated mortars required 47% of alkali solution to reach the workable flow (175 mm). The silicate activator was less workable, and required 60% of the solution to reach a lower flow diameter of 168 mm.

Physical properties and composition of the slag precursor. The particle size distribution was measured by laser diffraction using a Mastersizer 2000. This method measures the angular distribution and intensity of the light by particles in suspension and uses the Mie theory of diffraction in the prediction of laser particle size results. The specific surface area of the particles was measured with a Quantachrome Nova 4200e and the BET (Brunauer–Emmett–Teller) method which records the specific surface area based on the physical adsorption of gas molecules by the GGBS particles. The chemical composition of the GGBS was determined by an analysis of X-ray fluorescence (XRF) with ThermoFisher Scientific and Edwards Analytical using the Quant'X EDX spectrometer and the UniQuant analysis package as a percentage by oxides. The loss on ignition (LOI) was measured as weight loss by calcination.

The mineralogical composition and amorphous character of the precursors, was assessed with X-Ray Diffraction (XRD), using a Phillips PW1720 XRD with a PW1050/80 goniometer and a PW3313/20 Cu K-alpha anode tube at 40kV and 20mA.
As the slag was highly amorphous, thermal treatments to cause phase transformation (devitrification) were used to investigate the amorphous phases in the slag, using X-ray diffraction (XRD). The slag was also studied with differential scanning calorimetry (DSC) and thermal gravimetric analysis (TGA). DSC shows the thermal events (decomposition, combustion), as exothermic or endothermic peaks while TGA shows the weight loss over the temperature range.

Properties of the AA mortars. As aforementioned, the amount of alkali solution required for the GGBS to provide suitable workability for handling and placing (an approximate flow diameter of 175 mm) was measured with the initial flow diameter test using a flow table according to (EN 1015-3, 1999) [12]. The setting time was measured according to EN 196-3:2016 [13] which is designed for testing cement. The compressive strength was measured in accordance with EN1015-11, using a ZWICK 1474 machine of 100 kN loading capacity, at a loading rate of 10N/s. The results reported are the arithmetic mean of six tests. The microstructure of the materials was assessed with a scanning electron microscope (SEM) and a petrographic microscope after 28 days of curing. These qualitative analyses focussed on the cement matrix-aggregate interface. Thin sections sized approximately 2 cm^3 were prepared for SEM analysis. SEM micrographs were captured, between 5 and 10kV, using an SE2 detector with a Karl Zeiss Ultra FESEM microscope. The petrographic microscope was also used to study the matrix and the transition zone at the interface. Thin sections were cut from representative hand samples. They were polished to the standard thickness of c.20 microns and examined with a petrographic microscope in both transmitted and polarised light, with a mechanical rotating stage and low, medium and high-power objectives of 2×, 10×, 20x and 40× magnifications.

3. RESULTS AND DISCUSSION

3.1 Properties of the GGBS precursor.

The chemistry and mineralogy of the precursor (mainly its amorphous content), determine the formation of reaction products (alkaline cements) which consequently define the properties of the end materials. The fineness of the slag and its CaO content significantly affect the fresh and hardened properties of the AA materials [2].

Fineness. The fineness of the precursor is one of the main physical properties that influence reactivity and hence the mechanical properties of AAMs. In general, reactivity increases proportionally to fineness. In slags, fineness is a key factor influencing setting, strength development and the final microstructure of AAMs. The results (Table 2) evidence that the slag is ultrafine (1950 m^2/kg), considerably finer than the AA slags in the literature [4]. Over a certain threshold, fineness can have an adverse effect on strength due to a higher water demand. When activating slags, higher compressive strengths, especially at early ages, are achieved by increasing fineness (Brough and Atkinson, 2002; Križan et al. 2005 in [2]). However, increasing slag fineness can cause significant shortening of the setting time [14,15]. Wang and Scrivener[14] and Puertas [15] suggest that the optimal fineness lies between 400 and 550 m^2/kg.

Table 2. Specific surface area and particle size of the GGBS.

	Specific surface area (SSA) m^2/kg	Particle size			
		Mean µm	D90 µm	D50 µm	D10 µm
GGBS	1950	Range 0.25 to 75			
		18.00	31.62	11.67	2.35
CEM II	1880	-			

Chemical composition. The chemical composition (Table 3) evidences that the GGBS has a basicity (CaO+ MgO / SiO_2) of 1.56, hence it is basic (>1). The more basic the slag the greater its hydraulic activity in the presence of alkali activators (Moranville-Regourd 1988 in [4]). In general, glassy slags with CaO/SiO_2 ratios between 0.50 and 2.0, and Al_2O_3/SiO_2 ratios between 0.1 and 0.6 are considered suitable for alkali-activation [3]. The ratios in the slag investigated are 1.41 and 0.34 respectively, therefore suitable for alkali activation. In addition, the slag complies with the standard chemical requirements for the use of slags in concretes mortars and grouts (Table 4).

Table 3. Chemical composition as a percentage by weight. [a] same GGBS analysed by [16].

	SiO_2	Al_2O_3	CaO	Fe_2O_3	Na_2O	K_2O	MgO	P_2O_5	SO_3	Cl	TiO_2	MnO	LOI %	
													450 °C	1000 °C
GGBS	31.71	10.83	44.9	0.51	0.03	0.71	7.50	0.42	2.08	0.03	0.95	0.17	0.41	-0.77
GGBS[a]	34.14	13.85	39.27	0.41	0	0.26	8.63	-	2.43	-	0.54	0.25		
Mean	32	12	42	0.45	0.03	0.5	8	0.42	2.2	0.03	0.75	0.2		

Table 4. Compliance of the GGBS with chemical standard requirements.

	% SO_3 - S^{2-}	MgO (%)	Cl^-	LOI (%)	Fineness m^2/kg
EN 15167-1: GGBS requirements for use in concretes, mortars and grouts	≤ 2-2.5	≤ 18	≤ 0.10	≤ 3	≥275
GGBS	2.2	8	0.03	0.41	1950

Mineral composition and amorphousness. The mineralogy of the precursor, mainly its amorphous or vitreous phase content determines the formation of alkaline cements which, in slags, are mainly C-A-S-H gels that define the mechanical strength and durability of the resultant materials. The X-Ray diffraction pattern (figure 1) shows that the GGBS is largely amorphous with no crystalline phases evident. Therefore, the silica and alumina in the slag are reactive.

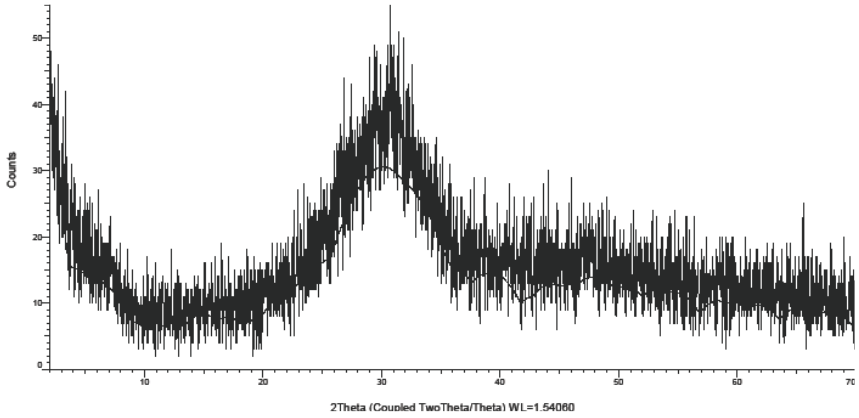

Figure 1. XRD trace of the slag with no crystalline phases and a marked halo which indicates that the slag is highly amorphous.

Devitrification. The thermal treatment applied to investigate the amorphous phases in the GGBS caused phase transformation. According to the results, the transformation of the amorphous phases into crystalline ones begins at approximately 500°C. The glassy nature of the unheated slag can be evidenced in the XRD trace with an extended halo (figure 1).
At 500°C, the GGBS is still mostly glass, but a small amount of crystalline merwinite $Ca_3Mg(SiO_4)_2$ has begun to form (figure 2). At 800°C (figure 3) there is a significant crystalline fraction: the amount of merwinite has increased and significant gehlenite Ca_2Al [$AlSiO_7$] has formed. At 1000 °C, the GGBS is crystalline (figure 4). The new crystalline phases are a representation of the amorphous phases which existed in the material, and include merwinite Ca_3Mg $(SiO_4)_2$ and gehlenite Ca_2Al [$AlSiO_7$]. Merwinite begins to appear at 500°C and it is abundant at 800°C, however over this temperature, it is no longer stable and transforms into gehlenite and, at 1000°C, it has completely disappeared (figure 4). This mineral composition agrees with other slags in the literature, as crystalline slags contain melilite as the main constituent, and melilite is a series of isomorphous solid solutions of which one of the two end members is gehlenite (Moranville-Regourd 1988 in [4]).

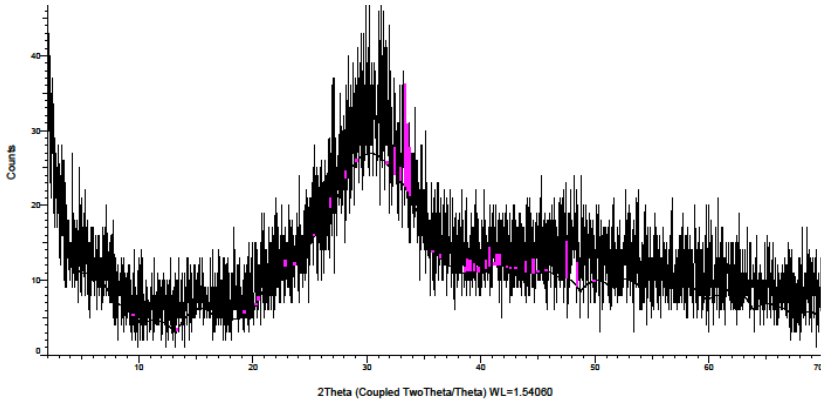

Figure 2. XRD trace of the slag at 500°C, the halo indicates that the slag is highly amorphous but a small amount of crystalline merwinite $Ca_3Mg(SiO_4)_2$ has begun to form.

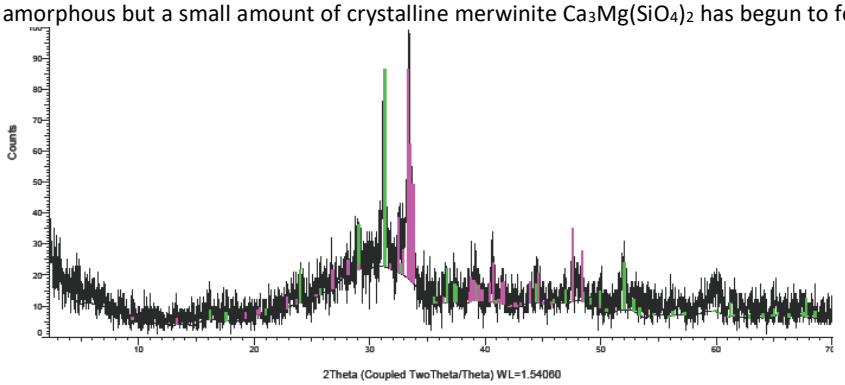

Figure 3. XRD trace of the slag at 800°C, the amount of merwinite has increased and gehlenite Ca_2Al [$AlSiO_7$] begins to form.

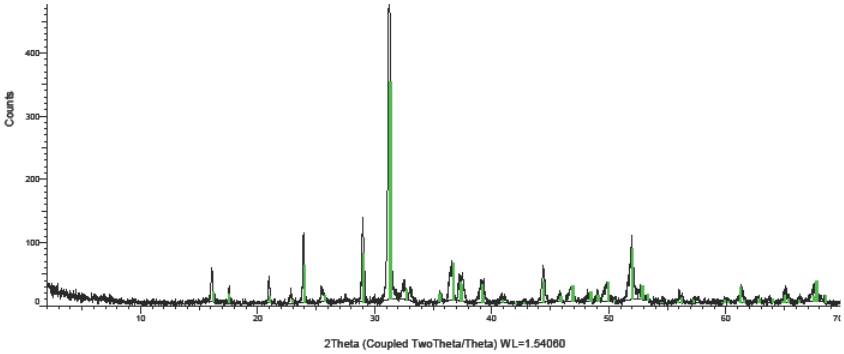

Figure 4. At 1000°C, the GGBS is completely devitrified, only gehlenite is stable, and merwinite has transformed into crystalline gehlenite.

The glass content of the GGBS at increasing temperature was calculated, as a percentage, based on the background area determined by the lifting of the difractogram's baseline between 15 and 35 (2Θ) which indicates the presence of amorphous materials (Table 5). The relative amounts of the crystalline phases were calculated using the relative intensities of their main reflexions: merwinite: 2Θ=33.38 with d-spacing= 2.68; and gehlenite: 2Θ=31.20 with d-spacing= 2.85 Å.

Table 5. Mineral composition and amorphousness of the GGBS. (*) calculated using the intensities of main reflexions: merwinite: 2Θ=33.38 / d-spacing= 2.68; gehlenite: 2Θ=31.20 / d-spacing= 2.85 Å.

Material	% Glass	% Crystalline	Mineral composition
GGBS 0°C	>90	<7	Glass. No crystals recorded.
GGBS 500°C	80-85	>7	Glass + traces of crystalline phases.
GGBS 800°C	c.11	50*	Merwinite $Ca_3\,Mg\,(\,Si\,O_4\,)_2$ Gehlenite $Na_{0.05}\,Ca_{1.96}\,Mg_{0.24}\,Fe_{0.12}\,Al_{1.25}\,Si_{1.39}\,O_7$
		38*	
GGBS 1000°C	<7	>90	Gehlenite $Na_{0.05}\,Ca_{1.96}\,Mg_{0.24}\,Fe_{0.12}\,Al_{1.25}\,Si_{1.39}\,O_7$

Thermal analyses. The slag was studied with differential scanning calorimetry (DSC) and thermal gravimetric analysis (TGA) (figure 5). DSC indicates thermal events (crystallization, dehydroxilation, combustion), as exothermic or endothermic peaks while TGA shows the weight loss over the temperature range.

According to the DSC results, the GGBS releases heat up to approximately 500°C (a progressive exothermic DSC curve can be observed between 0 and c.500°C). The devitrification test demonstrates that, during this heat evolution, only a small amount of crystals appear and no major changes occur in the GGBS which remains amorphous (figure 1-2 and table 5).

After 500°C, the DSC curve becomes endothermic, and the GGBS keeps absorbing heat until it reaches c. 800°C. Endothermic peaks are usually associated with a decomposition reaction. The devitrification test proves that the steady heat absorbed between 500 and 800°C is due to the decomposition of most of the glass to form crystalline merwinite and gehlenite (figure 3 and table 5).

As indicated by the phase evolution during devitrification, the marked exothermic peak at approximately 850°C likely corresponds to the transformation of merwinite into gehlenite, while the steady endothermic branch that follows (up to 1000°C) probably corresponds to the decomposition of the remining glass into crystalline gehlenite (figure 4 and table 5).

The main events agree with (Moranville-Regourd 1988 [4]) who identified main endothermic peaks at 800°C and 1000°C, and attribute this to the devitrification of the mineral phases in the GGBS. When compared with the heat evolution in other GGBS [17], the crystallization reactions are more progressive and steady, taking place over a longer temperature range rather than suddenly at a specific temperature.

The TGA measures changes in mass such as dehydration, decarbonation or oxidation. The mass of the GGBS remains more or less constant up to 1000°C, with a slight mass loss (1%) and a final slight mass increase. This indicates that the GGBS does not include either constitutional water or organic carbon or carbonates, supporting the LOI results (Table 3) and the chemical and mineralogical analyses (Tables 3 and 5). After reaching approximately 850°C, the GGBS gains a slight mass. The devitrification experiment indicates that this is probably due to the conversion of merwinite $Ca_3Mg\,(SiO_4)_2$ into denser gehlenite $Ca_2Al\,[AlSiO_7]$ (Table 5).

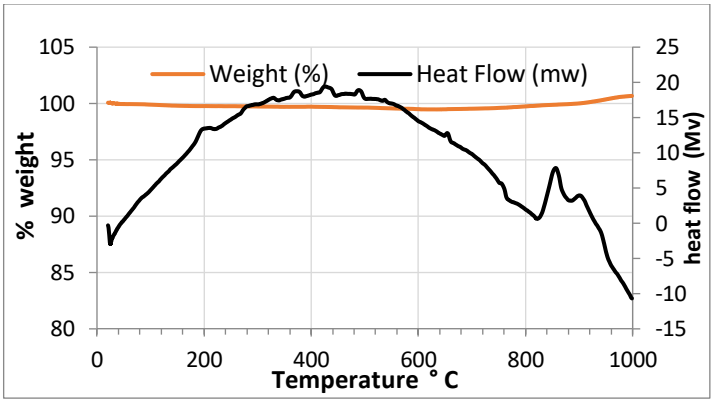

Figure 5. TGA / DSC analysis of the GGBS.

3.2 Properties of the AA mortars

Setting times. All the activators produced similar setting times except for the NaOH activated slag which requires a significantly longer time to finally set (Table 6). The results agree with others reported in the literature (Table 6). Previous authors have reported that, when finer than 450 m^2/kg, AA slag binders set in 1-3 minutes and hence the material is impossible to pour (Talling and Brandstetr in [3]). However, despite the slag being ultrafine, the setting times are over one hour for all the activators. According to Anderson and Gram [18], the fineness of the slag does not affect the setting time significantly between values ranging from 350-530 m^2/kg. However, the setting times are much shorter when fineness increases. The setting time also depends on the basicity of the slag. Basicity= CaO+ MgO / SiO_2. Higher basicity will likely result in shorter setting times regardless of the activator [19].

Table 6. Setting time for alkali activated slags.

Activators	Initial time: t_i	Final time: t_f	▲t= t_i - t_f	Slag properties	
				Fineness (m^2/kg)	Basicity
Na_2SiO_3	1h 11 min	1h 31 min	20 min	1950	1.56
Na_2SiO_3/NaOH	1h 8 min	1h 26 min	18 min		
NaOH	1h 15 min	2h 8 min	53 min		
Fernández-Jiménez and Puertas [20,21]					
Na_2SiO_3	1h 16 min	1h 46 min	20 min	460	1.51
80%Na_2SiO_3/20%NaOH	1h 15 min	1h 55 min	25 min		
NaOH	2h 45 min	3h 50 min	30 min		
80%NaOH/20%Na_2SiO_3	1h 10 min	1h 40 min	20 min		
Andersson & Gram [18]					
Na_2SiO_3	2h 20min	4h 45min	2h 25min	550	1.40
NaOH	3h 40min	4h 40 min	1h		

Mechanical Strength. The Na_2SiO_3 + NaOH activated slags generally achieve the greatest compressive and flexural strengths at all ages (Table 7 and Figures 6-7) agreeing with Fernández–Jiménez et al. [5]. Using this activator, rising the curing temperature enhances both flexural and compressive strengths mainly at early ages. This agrees with other authors stating an enhancement of mechanical strength, with increasing curing temperature, in Na_2SiO_3 + NaOH activated slags at early ages [5, 6, 20, 21, 22, 23]. Bakharev et al. [6] observed that curing at 70ºC accelerates early strength development but, after 28 days, the strength was 35 to 45% lower than that of ambient cured specimens.

Table 7. Compressive and flexural strength of the alkali-activated slag (MPa). COVs- coefficients of variation.

	Na_2SiO_3/NaOH activated GGBS				NaOH activated GGBS				Na_2SiO_3 activated GGBS			
	Flexural strength		Compressive strength		Flexural strength		Compressive strength		Flexural strength		Compressive strength	
	COVs = 0.05-0.13		*COVs =0.10-0.49*		*COVs =0.05-0.58*		*COVs =0.09-0.23*		*COVs =0.03-0.41*		*COVs =0.05-0.29*	
	60°C	20°C	60°C	20°C	60°C	20°C	60°C	20°C	60°C	20°C	60°C	20°C
3 day	7.31	0.66	44.11	1.88	1.75	3.33	8.56	8.09	0.81	0.28	1.30	0.60
7 day	7.10	3.51	34.38	12.08	1.15	3.07	7.53	8.77	0.93	0.70	1.50	1.31
28 day	7.09	6.12	33.69	25.70	1.65	0.77	12.03	17.56	3.25	1.89	2.92	5.21

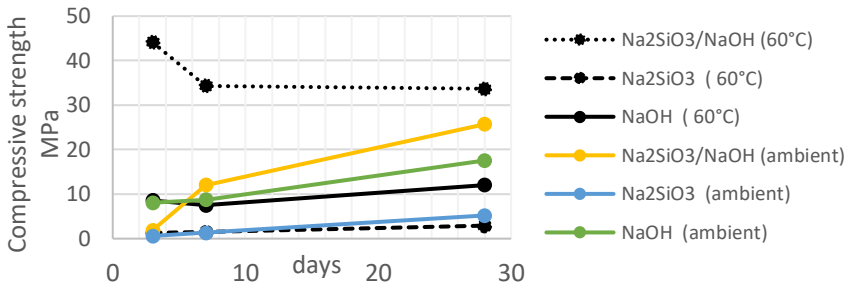

Figure 6. Compressive strength of the alkali-activated GGBS ambient and oven cured.

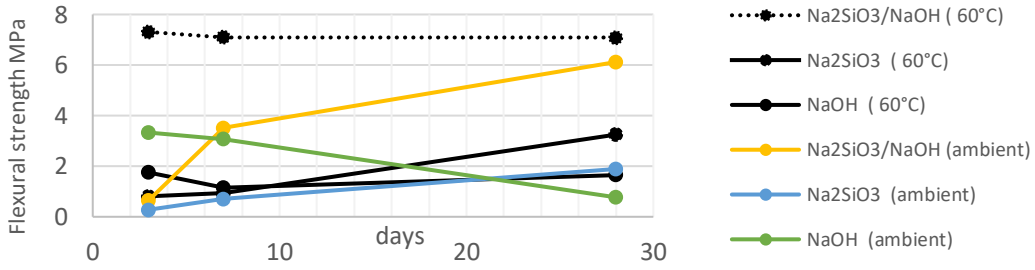

Figure 7. Flexural strength (MPa) of the alkali-activated GGBS ambient and oven cured.

On the contrary, rising the curing temperature lowers the ultimate compressive strength of the NaOH and Na_2SiO_3 activated slags. This disagrees with Bakharev et al. [6] who note that 60°C is the best temperature for curing Na_2SiO_3-activated slags. However, it agrees with Fernández–Jiménez et al. [20,21] who note that an increase of curing temperature lead to a decrease in strength for NaOH-activated slags at all ages. The effect of the temperature is not so clear on the flexural strength (figure 7) when the NaOH and the Na_2SiO_3 activators are used separately, as the ultimate flexural strength of the Na_2SiO_3 slag increases with rising curing temperature. The 0.77 MPa result of the NaOH activated slag is unreliable, and likely due to a defective specimen with microcracks.

The Na_2SiO_3 activated slags result in poor strengths disagreeing with previous studies that found silicate activated slags often develop the highest strength [6, 10, 20-24]. The reason for the low strength is likely the high Na_2O content in the specimens, as the optimum quantity of Na_2O lies between 3-6% by mass of slag and the materials tested are well over this threshold [4].The appearance of efflorescence (figure 8) in some of the specimens agrees with high Na_2O content. The appearance of alkali carbonate efflorescence due to the leaching of alkalis and their reaction with the CO_2 in the air has been previously reported in the literature [1]. The strengths of the Na_2SiO_3 + NaOH activated slags are lower than others previously reported. This can be due to the ultrafine nature of the slag particles: It has been reported that an increment in the specific surface area of the slag has a negative effect on strength when the activators are Na_2SiO_3 + NaOH [21]. The NaOH activated slags also result in poor strength, lower than the values typically reported in the literature (under the <20MPa reported for moist or water cured specimens by Talling and Krivenko [25]. The lower strength of the NaOH activated slags can be due to using an alkalinity too high for the highly reactive nature of this slag. The appearance of microcracks in some of the specimens also agrees with the high alkalinity in the material (figure 9).

Figure 8. Efflorescence in Na_2SiO_3 activated GGBS cured in ambient conditions probably due to a high Na_2O content in the mix.

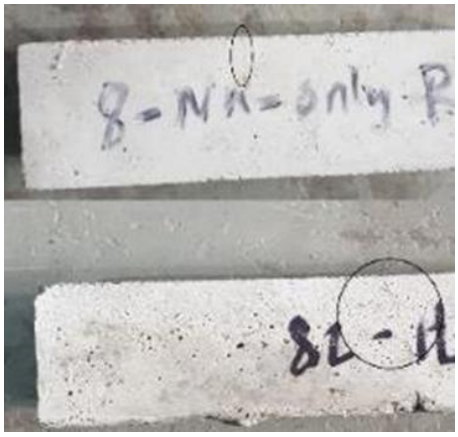

Figure 9. Microcracks in a NaOH-activated GGBS specimen cured in ambient conditions that may be related to the high molarity of the NaOH solution.

The effect of increasing the curing temperature for each of the activators is shown in detail in the figures 10-12. As it can be seen from these figures, increasing the curing temperature, enhances strength when Na_2SiO_3 / NaOH is the activator (most significantly at early ages) (figure 10) but lowers the ultimate compressive strength when the NaOH and Na_2SiO_3 activators are used separately (figures 11-12). The effect of increasing the curing temperature is not so clear on the flexural strengths of the NaOH and Na_2SiO_3 activated slags (figures 11-12), but the ultimate flexural strength of the Na_2SiO_3 activated slag seems to increase significantly with rising curing temperature.

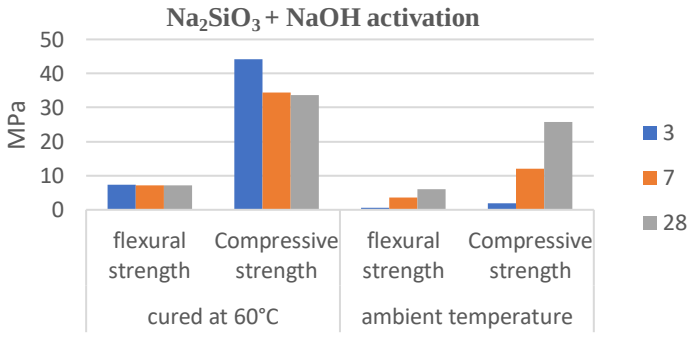

Figure 10. Effect of curing temperature on the strength development of the GGBS activated with Na_2SiO_3 / NaOH. Legend: 3, 7, 28 days.

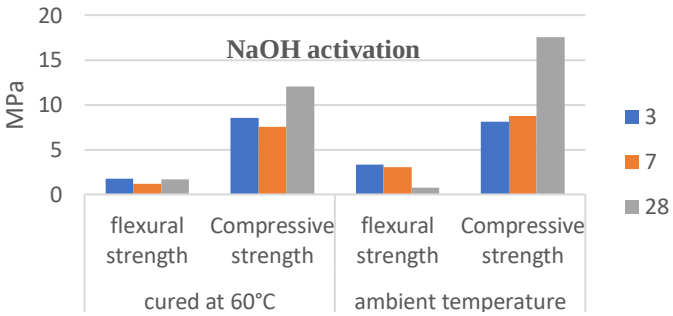

Figure 11. Effect of curing temperature on the strength development of the GGBS activated with NaOH.

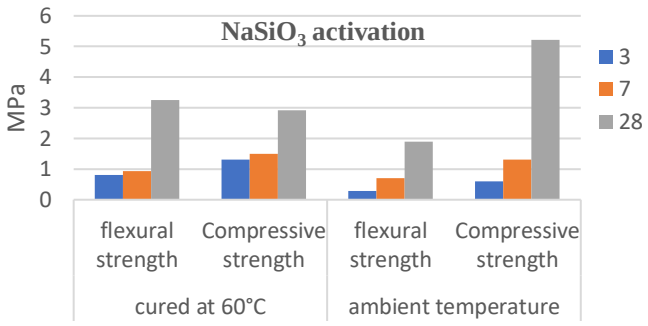

Figure 12. Effect of curing temperature on the strength development of the GGBS activated with Na_2SiO_3.

Microstructure. The Na_2SiO_3+NaOH activated GGBS showed the best mechanical strength. Therefore, its microstructure was investigated with petrography and SEM analyses. The microscope analyses show a dense microstructure where pores are virtually absent. Given the restricted and qualitative nature of these techniques, no direct correlation could be established between the microscopic analyses and the strength results. However, the results evidenced that the microstructure of the material is sound, the aggregate and the GGBS are evenly distributed and the bond at the interface is continuous (figure 13-16). In the ambient cured materials (figure 13), the petrographic microscope showed abundant unreacted GGBS grains in an opaque groundmass with occasional patches of cement. However, in the oven cured materials (figure 14), the structure of the matrix is more crystalline and the GGBS particles often show reaction and the formation of cementing hydrates. The petrographic microscope did not provide enough resolution to identify the nature of the hydrates. No alkali-aggregate reactions (AAR) or alkali-silica reactions (ASR) were evident (figure 15-16), and none of the aggregate had reacted with the alkaline binder, not even the microsilica (chert) grains. However, 28 days is likely too early to expect any AAR or ASR.

The SEM analyses confirmed the petrographic analysis results. Furthermore, the SEM showed tiny micro-cracks in the Na_2SiO_3+NaOH materials that were invisible with the naked eye and with the resolution of the petrographic microscope (figure 17). The appearance of cracking due to drying shrinkage has been reported to increase as the lime content in the system lowers [1]. Hence the high Ca content of this slag has probably contributed to the sound microstructure of the materials.

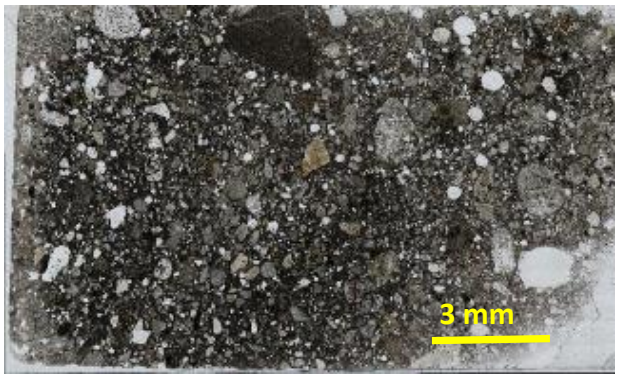

Figure 13. Na_2SiO_3 + NaOH activated GGBS cured at ambient temperature where abundant fine GGBS is still evident in the matrix.

Figure 14. Na_2SiO_3 + NaOH activated GGBS cured at 60°C shows stronger reaction, a more homogeneous matrix where much of the GGBS has become cement. Scale as in figure 13.

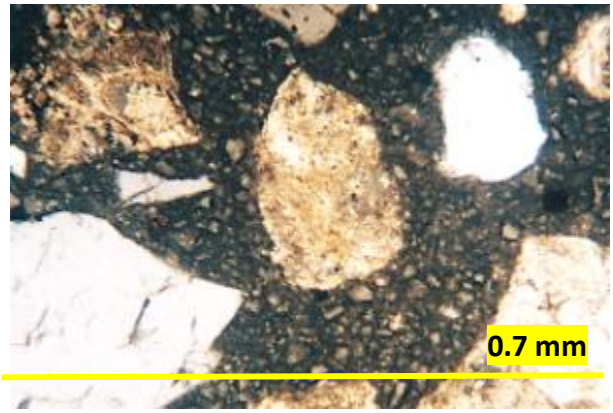

Figure 15. Representative image of the Na_2SiO_3 + NaOH activated GGBS, cured at ambient temperature, with abundant unreacted GGBS in the matrix and sound aggregate with no evidence of alkali reaction. X20 polarised light.

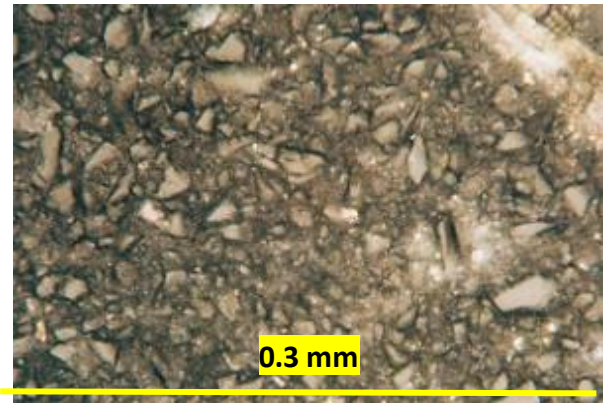

Figure 16. Detail of the GGBS reaction and the cement formed by alkali reaction in the oven-cured, Na_2SiO_3 + NaOH- activated, GGBS matrix. X40 polarised light.

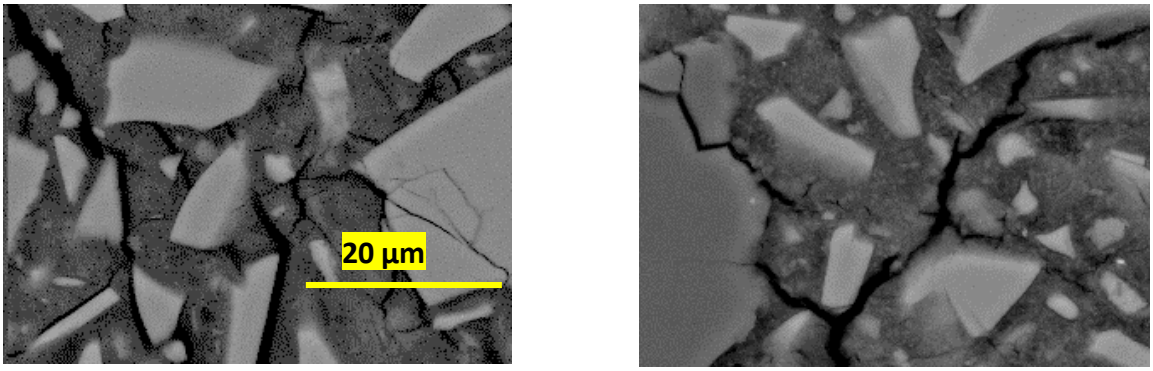

Figure 17. SEM images of the Na_2SiO_3/NaOH activated GGBS, cured at ambient temperature, showing fractures and abundant unreacted GGBS. Scale as in left figure.

CONCLUSION

This paper investigates the possibility of producing building materials by activating an Irish slag with a range of alkali metal activators. The GGBS shows outstanding qualities for the production of AA binders being highly reactive: it is ultra-fine (SSA=1950 m^2/kg) and basic (CaO+ MgO / SiO_2 =1.56 basicity). Furthermore, it is highly amorphous, and has a CaO/SiO_2 ratio of 1.41 and a Al_2O_3/SiO_2 ratio of 0.34 which are considered suitable for alkali-activation. The devitrified mineral composition agrees with that of other active slags in the literature, comprising melilite as the main constituent, in an isomorphous solid solution where the other end member is gehlenite. In addition, the GGBS complies with the standard requirements for use of slags in concretes, mortars and grouts. Cracking due to drying shrinkage is one of the challenges of AA materials. However, it seems that the high Ca content of this slag contributes to the sound microstructure of the materials, and the low drying shrinkage cracking. Therefore, the GGBS can be successfully used for the production of AA materials.

Despite being ultra-fine, the GGBS shows feasible setting times and minimal loss of workability. The rheology and setting times of the materials produced are within practical limits, comparable to values obtained for other slags by previous authors. The strengths are lower than those reported in the literature, however, the Na_2SiO_3+NaOH activated GGBS shows significant values, suitable for a wide range of applications. The main reason for the strength loss when using the Na_2SiO_3 activator alone is likely an excessive $\%Na_2O$ by mass of slag (the ultrafine character of the slag would require a lower $\%Na_2O$), while the reason for the strength loss when the NaOH activator is involved is an excessive alkalinity, produced by an undue high molarity of the NaOH solution. As evidenced by the strength results and the microstructural analyses, rising curing temperature improves the microstructure and the mechanical properties of the Na_2SiO_3+NaOH activated GGBS. From the above, it can be concluded that the quality of the activator determines the strength of AA slag which agrees with previous authors. This particular GGBS seems too fine for a successful activation with Na_2SiO_3 alone, and too reactive for high alkali hydroxide concentrations. It seems from the results, that the best activator for this slag is a combination of alkali silicate and a (low molarity i.e. <6) alkali hydroxide.

Acknowledgements

The authors thank the Government of Saudi Arabia, Technical & Vocational Training Corporation and the Saudi Arabian Cultural Bureau for their support and for financing the project. Also, J. Reddy, Senior Manager of Ecocem, R. Goodhue and T. Dornan of TCD Geochemistry; A. Rafferty, of the Centre for Research on Adaptive Nanostructures and Nanodevices, TCD; O. Clarkin, Dublin City University, and J. Canavan, Geography Department, TCD, for their assistance with the analyses. Finally, we thank our colleagues in the Civil Engineering laboratories M. Gilligan and E. Dunne, and in particular, M. Grimes, our Chief Technician D. McAuley and P. Veale for their assistance during testing.

References

[1] Shi C., Krivenko P. V. & Roy D. (2006) Alkali-activated cements and concretes. Taylor & Francis. London, New York.

[2] Pacheco-Torgal, F., Labrincha, J., Leonelli, C., Palomo, A., & Chindaprasit, P. (Eds.). (2014). Handbook of alkali-activated cements, mortars and concretes. Elsevier.

[3] Provis, J. L., & Van Deventer, J. S. (Eds.). (2013). Alkali activated materials: state-of-the-art report, RILEM TC 224-AAM (Vol. 13). Springer Science & Business Media.

[4] Lea's Chemistry of Cement and Concrete. 4th Edition (1988) Ed. P. Hewlett, Butterworth-Heinemann- Elsevier.

[5] Fernández-Jiménez, A., Palomo, J. G., & Puertas, F. (1999). Alkali-activated slag mortars: Mechanical strength behaviour. *Cement and Concrete Research*, *29*(8), 1313–1321. https://doi.org/10.1016/S0008-8846(99)00154-4

[6] Bakharev, T., Sanjayan, J. G., & Cheng, Y. B. (2000). Effect of admixtures on properties of alkali-activated slag concrete. *Cement and Concrete Research*, *30*(9), 1367–1374. https://doi.org/10.1016/S0008-8846(00)00349-5

[7] Liew, Y. M., Heah, C. Y., Mohd Mustafa, A. B., & Kamarudin, H. (2016). Structure and properties of clay-based geopolymer cements: A review. *Progress in Materials Science*, *83*, 595–629. https://doi.org/10.1016/j.pmatsci.2016.08.002

[8] Brough, A. R., & Atkinson, A. (2002). Sodium Silicate-Based, Alkali-Activated Slag Mortars - Part I. Strength, Hydration and Microstructure. *Cement and Concrete Research*, *32*, 865–879. https://doi.org/10.1016/S0008-8846(02)00717-2

[9] Bakharev T, Sanjayan, J. G., & Cheng, Y. B. (1999). Alkali activation of Australian slag cements. *Cement and Concrete Research*, *29*(1), 113–120. https://doi.org/10.1016/S0008-8846(98)00170

[10] Altan E. and Erdoğan S. T. (2012). Alkali activation of a slag at ambient and elevated temperatures, *Cement and Concrete Composites,* Volume 34, Issue 2, 131-139, https://doi.org/10.1016/j.cemconcomp.2011.08.003.

[11] Das, S. K., Banerjee, S., & Jena, D. (2013). A Review on Geo-polymer Concrete. *International Journal of Engineering Research & Technology 2*(9), 2785–2788.

[12] EN 1015-3 (1999). Methods of Test for Mortar for Masonry. Part 3. Determination of consistence of fresh mortar (by flow table).

[13] EN 196-3 (2016). Methods of testing cement. Part 3. Determination of setting times and soundness.

[14] Wang, S. D., & Scrivener, K. L. (1995). Hydration products of alkali activated slag cement. *Cement and Concrete Research*, *25*(3), 561–571. https://doi.org/10.1016/0008-8846(95)00045-E

[15] Puertas, F. (1995). Cementos de escorias activadas alcalinamente: Situación actual y perspectivas de futuro. *Materiales de Construcción,* 45(239), 53-64.

[16] Walker, R. & Pavía, S. (2010). Behaviour and Properties of Lime-Pozzolan Pastes. *8th International Masonry Conference, Dresden, July 2010*, 353–362.

[17] Sha, W., & Pereira, G. B. (2001). Differential scanning calorimetry study of ordinary Portland cement paste containing metakaolin and theoretical approach of metakaolin activity. *Cement and Concrete Composites*, 23(6), 455-461.

[18] Andersson, R., & Gram, H. E. (1987). Properties of alkali activated slag concrete. *Nordic concrete research*, (6), 7-18.

[19] Krivenko, P. V. (1994). Influence of physico-chemical aspects of early history of a slag alkaline cement stone on stability of its properties. In Proc. of 1st International Conference on Reinforced Concrete Materials in Hot Climates.

[20] Fernández-Jiménez, A., & Puertas, F. (2001). Setting of alkali-activated slag cement. Influence of activator nature. *Advances in Cement Research*, 13(3), 115-121.

[21] Fernández-Jiménez, A., & Puertas, F. (2003). Effect of activator mix on the hydration and strength behaviour of alkali-activated slag cements. *Advances in cement research*, 15(3), 129-136.

[22] Atiş, C.D., Bilim, C., Çelik, Ö., Karahan O., (2009) Influence of activator on the strength and drying shrinkage of alkali-activated slag mortar, *Construction and Building Materials* 23 548–555, doi:http://dx.doi.org/10.1016/j.conbuildmat.2007.10.011.

[23] Krizan, D. & Zivanovic, B., (2002) Effects of dosage and modulus of water glass on early hydration of alkali–slag cements, *Cement Concrete Research* 32 1181–1188, doi:http://dx.doi.org/10.1016/S0008-8846(01)00717-7.

[24] Burciaga-Díaz, O. & Escalante-García, J. I. (2013). Structure, mechanisms of reaction, and strength of an alkali-activated blast-furnace slag. *Journal of the American Ceramic Society*, 96(12), 3939-3948.

[26] Talling, B. & Krivenko, P. (1996) Alkali activated slag cements from research to practice. SCI meeting on AA slag cements London 17 June 1996.